Perspectives on preservation of physical properties through optimization

SAND2013-8197P

Pavel Bochev Denis Ridzal Kara Peterson

Sandia National Laboratories

in collaboration with

Mikhail Shashkov (LANL)

High-Resolution Mathematical and Numerical Analysis of Involution-Constrained PDEs
Oberwolfach, September 15-20, 2013

Sandia National Laboratories is a multi-program laboratory managed and operated by Sandia Corporation, a wholly owned subsidiary of Lockheed Martin Corporation, for the U.S. Department of Energy's National Nuclear Security Administration under contract DE-AC04-94AL85000.

The larger picture

Atomistic-to-continuum coupling

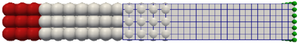

ATOMISTIC MODEL FINITE ELEMENTS

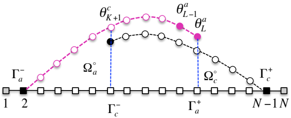

Optimization-based modeling (DOE/ASCR)

$$\min_u \|u - u^T\| \quad \text{s.t. } L^h(u) \geq 0$$

Operator splitting and solver synthesis

Study	Fixed diffusion: 10^{-8}			Fixed grid size: 128		
	64	128	256	10^{-2}	10^{-4}	10^{-8}
OBM-ML^{SGS}	**114**	**97**	**77**	**62**	**97**	**97**
ML^{ILU}	71	196	—	9	96	196
BAMG	72	457	—	7	33	457

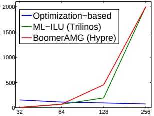

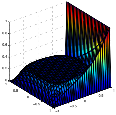

Feature-preserving solution transfer

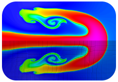

ALE

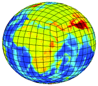

SEMI-LAGRANGIAN

The larger picture

Atomistic-to-continuum coupling

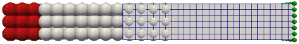

ATOMISTIC MODEL FINITE ELEMENTS

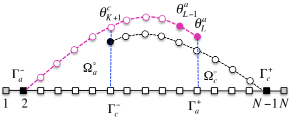

Operator splitting and solver synthesis

Study	Fixed diffusion: 10^{-8}			Fixed grid size: 128		
	64	128	256	10^{-2}	10^{-4}	10^{-8}
OBM-ML^{SGS}	**114**	**97**	**77**	**62**	**97**	**97**
ML^{ILU}	71	196	—	9	96	196
BAMG	72	457	—	7	33	457

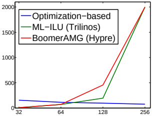

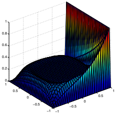

Optimization-based modeling (DOE/ASCR)

$$\min_u \|u - u^T\| \quad \text{s.t.} \quad L^h(u) \geq 0$$

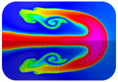

ALE

Feature-preserving solution transfer

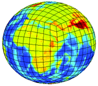

SEMI-LAGRANGIAN

Solution transfer

Scalar mass-density remap

Flux form of optimization-based remap

- Mathematical formulation
- Theoretical properties and benefits
- Algorithm and computational cost

Mass form of optimization-based remap

- Mathematical formulation
- Algorithm and computational cost

New directions and technology transfer

- Adaptable targets and smoothness indicators
- High-order remap: BLAST, HOMME
- Tensor remap: ALEGRA

Solution transfer

Scalar mass-density remap

Flux form of optimization-based remap

Mathematical formulation

Theoretical properties and benefits

Algorithm and computational cost

Mass form of optimization-based remap

Mathematical formulation

Algorithm and computational cost

New directions and technology transfer

Adaptable targets and smoothness indicators

High-order remap: BLAST, HOMME

Tensor remap: ALEGRA

Solution transfer

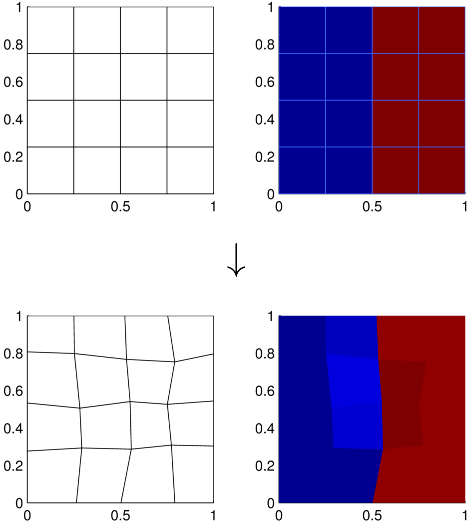

Solution transfer

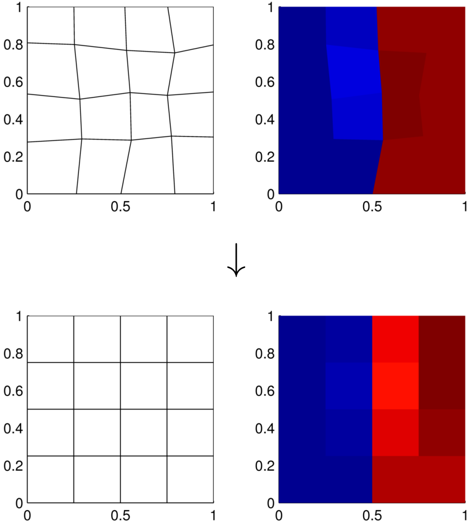

Solution transfer

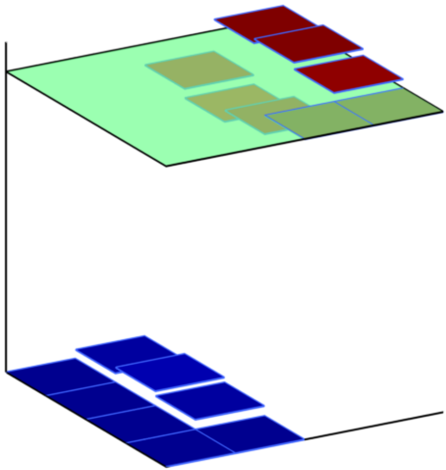

Solution transfer

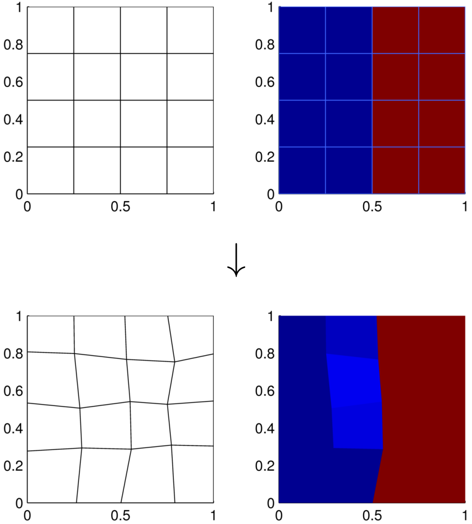

Solution transfer

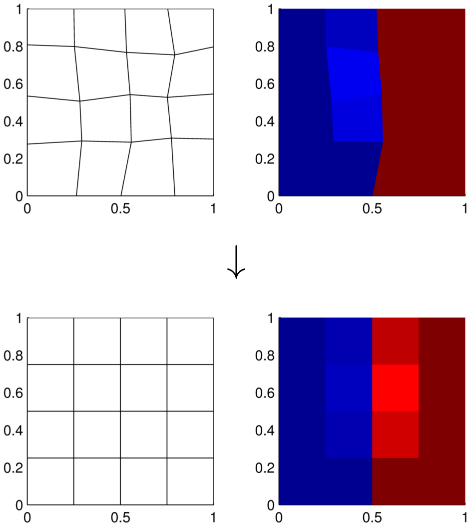

Solution transfer

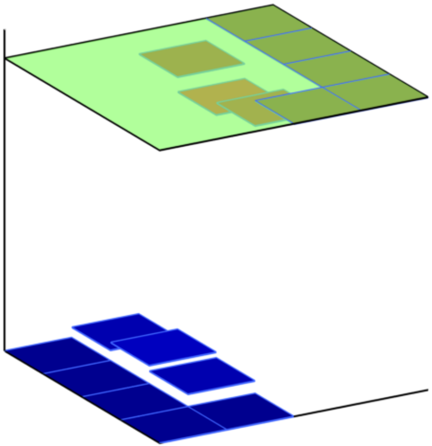

Solution transfer

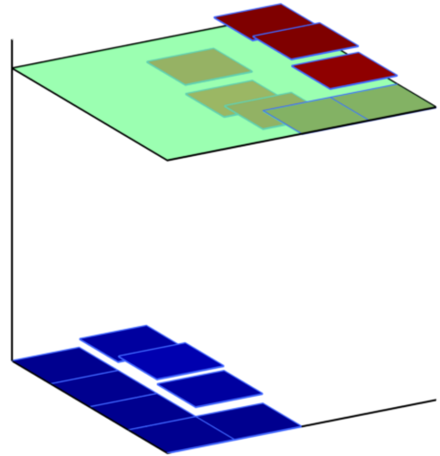

Solution transfer

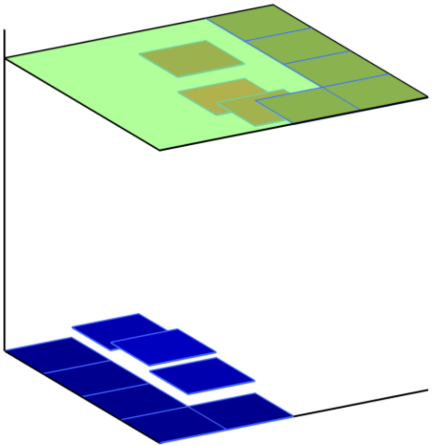

Solution transfer

Given: Discrete representation $\mathbf{f_A}$ of function $\mathbf{f}$ on mesh $\mathbf{A}$.

Find: *Accurate* discrete representation $\mathbf{f_B}$ of $\mathbf{f}$ on mesh $\mathbf{B}$, subject to physical constraints:

- conservation of mass, energy, etc.
- preservation of monotonicity
- physically meaningful ranges for variables: density ≥ 0, concentration $\in [0, 1]$

Critical task in computational science:

- shock-hydrodynamics: ALEGRA, BLAST, etc.
- tracer transport: sea ice – CICE, atmosphere – HOMME, etc.
- mesh repair, rezone, untangling, reconnection, conservative regridding in, e.g., big ocean data
- transfer of simulation data between heterogeneous numerical models
- data visualization on arbitrary polygonal grids
- solution recovery for resilient computing

Mass-density remap

Given: *Old* mesh $C(\Omega)$ and mean density values ρ_i on old mesh cells c_i.

Find: Approximations $\widetilde{m}_i$ of masses on a *new* mesh $\widetilde{C}(\Omega)$ with cells $\widetilde{c}_i$,

$$\widetilde{m}_i \approx \widetilde{m}_i^{\text{exact}} = \int_{\widetilde{c}_i} \rho(\mathbf{x}) dV\,, \quad i = 1, \dots, C\,; \quad \textbf{subject to}$$

C1. Mass conservation: $\sum_{i=1}^{C} \widetilde{m}_i = \sum_{i=1}^{C} m_i = M\,.$

C2. Second-order accuracy: If $\rho(\mathbf{x})$ is a global linear function on Ω, then the mass approximations are exact,

$$\widetilde{m}_i = \widetilde{m}_i^{\text{exact}} = \int_{\widetilde{c}_i} \rho(\mathbf{x}) dV\,, \quad i = 1, \dots, C\,.$$

C3. Local bounds: The approximations of the mean density on the new cells, $\widetilde{\rho}_i = \widetilde{m}_i / V(\widetilde{c}_i)$, are bounded by the *old* neighborhood extrema

$$\rho_i^{\min} \le \widetilde{\rho}_i \le \rho_i^{\max}\,, \quad i = 1, \dots, C\,, \quad \text{or equivalently,}$$

$$\widetilde{m}_i^{\min} := \rho_i^{\min} V(\widetilde{c}_i) \le \widetilde{m}_i \le \rho_i^{\max} V(\widetilde{c}_i) =: \widetilde{m}_i^{\max}\,, \quad i = 1, \dots, C\,.$$

Some history

19xx–2010:

- Scalar remap is a long-studied problem.
- The constraints (C1)–(C3) are typically handled *by construction*:
  — a careful choice of variables in the remap scheme;
  — a special reconstruction procedure; and
  — a particular choice of 'limiter' (WIKIPEDIA: 15 slope limiters).
- Challenges: accuracy loss, mesh/cell dependence, robustness.
- **Game changer:**
  Flux-corrected remap (FCR), Shashkov et al., J. Comp. Phys., 2010.

2010–2012:

- We use globally constrained optimization to reconcile (C1)–(C3).
- A mathematically rigorous way to handle constraints.
- Elegant theory, and connections to methods like FCR.
- Improved accuracy; improved robustness; general applicability.

2012–2013:

- Optimization-based remap at the cost of conventional remap.

Solution transfer

Scalar mass-density remap

Flux form of optimization-based remap

Mathematical formulation
Theoretical properties and benefits
Algorithm and computational cost

Mass form of optimization-based remap

Mathematical formulation
Algorithm and computational cost

New directions and technology transfer

Adaptable targets and smoothness indicators
High-order remap: BLAST, HOMME
Tensor remap: ALEGRA

Flux form of OBR

1. Given the side-to-cell incidence matrix $\mathbf{D}$, or *discrete divergence*, define **mass update**

$$\widetilde{m} = m + \mathbf{D}F\,,$$

where F approximates the exact **fluxes** over the swept regions r_j,

$$F_j \approx F_j^{\text{exact}} = \int_{r_j} \rho(\mathbf{x})dV\,; \quad j = 1,\dots,S\,.$$

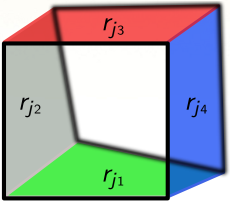

$\widetilde{m}_i = m_i + (\mathbf{D}F)_i =$
$m_i + \sum_{k\in\{j1,\dots,j4\}} \sigma_k F_k$

2. Compute **target** $F_j^{\mathrm{T}} := \displaystyle\int_{r_j} \rho^h(\mathbf{x})dV$, $j = 1,\dots,S$, for some density reconstruction $\rho^h(\mathbf{x})$ that is **exact for linear functions**. Solve:

$$\begin{cases} \underset{F}{\text{minimize}} \quad \frac{1}{2}\|F - F^{\mathrm{T}}\|_{\ell_2}^2 \qquad \text{subject to} \\ \widetilde{m}^{\min} \le m + \mathbf{D}F \le \widetilde{m}^{\max}\,. \end{cases}$$

Immediate properties

- **Local bounds are enforced directly:** $\widetilde{m}^{\min} \leq m + \mathbf{D}F \leq \widetilde{m}^{\max}$.
- **Mass conservation is implicit: follows from the divergence form**

$$\sum_{i=1}^{C} \widetilde{m}_i = \sum_{i=1}^{C} m_i + \underbrace{\sum_{i=1}^{C} (\mathbf{D}F)_i}_{=0,\ \text{divergence form}} = \sum_{i=1}^{C} m_i \,.$$

- **Theorem: Second-order accuracy.** A sufficient condition for OBR to recover linear densities **exactly** is that the centroid of any new cell remain in the **convex hull** of the centroids of its old neighbors.

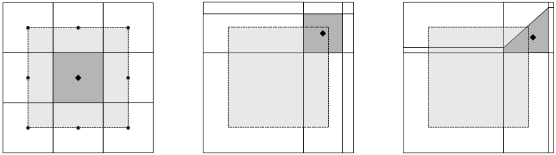

(a) original (b) admissible (c) inadmissible

Less restrictive!

- **Independent of dimension and cell topology.**
- **Separation of concerns: Optimally accurate and monotone!**

Relation to Flux-Corrected Remap (FCR)

Theorem. FCR can be formulated as a **global optimization problem**.

(1) The FCR cost function is equivalent to the OBR cost function.

(2) The FCR feasible set is **always a subset** of the OBR feasible set.

Compressive Mesh Motion

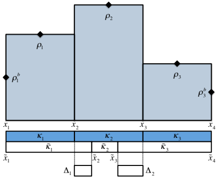

OBR Feasible Set

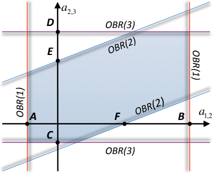

FCR Feasible Set

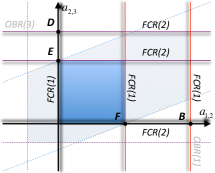

1. OBR preserves shape when FCR may not

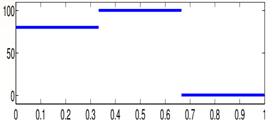

Original

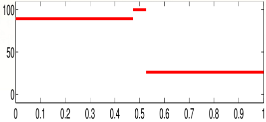

After a single OBR step

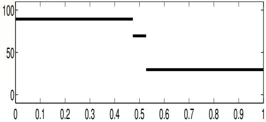

After a single FCR step

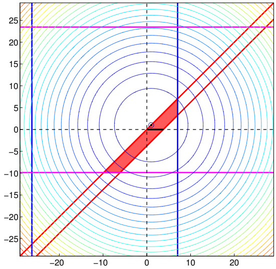

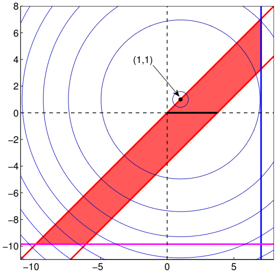

Level sets of the cost function and the feasible sets:

Red region = OBR feasible set; contains flux target $F^T = (1,1)$.

Solid horizontal segment (black) = FCR feasible set.

2. OBR preserves monotonicity when FCR may not

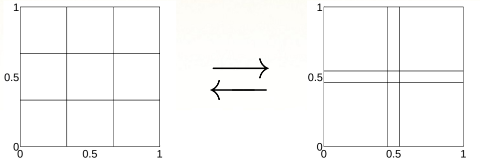

Figure: A 3×3 uniform initial grid (left pane) and the compressed “torture” grid (right pane) with a 4×4-fold compression of the middle cell.

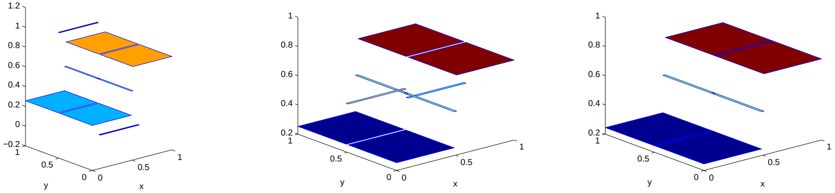

Figure: Linear density $\rho(x, y) = x$ remapped from the uniform 3×3 grid to the compressed “torture” grid with $\ell = 16$. Left to right: the donor-cell method, FCR, OBR. It is clear that OBR gives the best density approximation.

3. OBR is more accurate than FCR

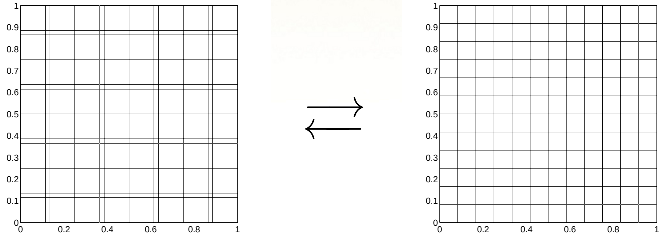

#cells	#remaps	L_1 err	L_2 err	L_∞ err	L_1 rate	L_2 rate	L_∞ rate
Remap of smooth (sine) density using OBR							
128×128	640	2.69e-04	3.65e-04	2.03e-03	—	—	—
256×256	1280	6.71e-05	9.08e-05	5.07e-04	**2.00**	**2.01**	**2.00**
512×512	2560	1.68e-05	2.27e-05	1.20e-04	**2.00**	**2.00**	**2.04**
1024×1024	5120	4.19e-06	5.66e-06	2.69e-05	**2.00**	**2.00**	**2.08**
Remap of smooth (sine) density using FCR							
128×128	640	2.81e-04	3.47e-04	1.23e-03	—	—	—
256×256	1280	9.23e-05	1.19e-04	5.14e-04	1.61	1.54	1.26
512×512	2560	3.65e-05	5.05e-05	2.50e-04	1.47	1.39	1.15
1024×1024	5120	1.69e-05	2.39e-05	1.24e-04	1.35	1.28	1.10

Flux-form OBR algorithm

How about speed?

Rather than solve

$$\begin{cases} \underset{F}{\text{minimize}} \quad \frac{1}{2}\|F - F^{\mathsf{T}}\|_{\ell_2}^2 \qquad \text{subject to} \\ \widetilde{m}^{\min} - m \le \mathbf{D}F \le \widetilde{m}^{\max} - m \end{cases}$$

directly, we solve its equivalent **dual reformulation**

$$\begin{cases} \underset{\lambda,\mu}{\text{minimize}} \quad \frac{1}{2}\|\mathbf{D}^T\lambda - \mathbf{D}^T\mu\|_2^2 - \langle \lambda, \widetilde{m}^{\min} - m - \mathbf{D}F^{\mathsf{T}}\rangle \\ \qquad\qquad -\langle \mu, -\widetilde{m}^{\max} + m + \mathbf{D}F^{\mathsf{T}}\rangle \\ \text{subject to} \quad \lambda \ge 0,\ \mu \ge 0\,. \end{cases}$$

Thus, we trade the complexity in the globally coupled inequality constraint for a more complex objective function.

Flux-form OBR algorithm

Some notation

- Define system matrix $\mathbf{H} \in \mathbb{R}^{2C\times 2C}$ and vector $b \in \mathbb{R}^{2C}$

$$\mathbf{H} = \begin{bmatrix} \mathbf{DD}^T & -\mathbf{DD}^T \\ -\mathbf{DD}^T & \mathbf{DD}^T \end{bmatrix} \qquad b = \begin{bmatrix} \mathbf{D}F^{\mathrm{T}} - \widetilde{m}^{\min} + m \\ -\mathbf{D}F^{\mathrm{T}} + \widetilde{m}^{\max} - m \end{bmatrix}$$

- Define the diagonal operator, $\mathrm{Diag} : \mathbb{R}^{2C} \to \mathbb{R}^{2C\times 2C}$, as

$$[\mathrm{Diag}(x)]_{ij} = \begin{cases} x_i & \text{when} \quad i = j \\ 0 & \text{''} \quad i \neq j \end{cases} .$$

- Define the operator $v : \mathbb{R}^{2C} \to \mathbb{R}^{2C}$ as

$$[v(x)]_i = \begin{cases} x_i & \text{when} \quad [\mathbf{H}x + b]_i \geq 0 \\ 1 & \text{''} \quad [\mathbf{H}x + b]_i < 0 \end{cases} .$$

- Define the operator $K : \mathbb{R}^{2C} \to \mathbb{R}^{2C\times 2C}$ as

$$[K]_{ii} = \begin{cases} 1 & \text{when} \quad [\mathbf{H}x + b]_i \geq 0 \\ 0 & \text{''} \quad [\mathbf{H}x + b]_i < 0 \end{cases} .$$

Flux-form OBR algorithm

Semismooth Newton

- It can be shown that under mild assumptions the solution of the bound-constrained problem is equivalent to the solution of the **piecewise differentiable system of equations**

$$\mathrm{Diag}(v(x))\,(\mathbf{H}x + b) = 0\,.$$

- Apply Newton's method to the nonlinear system by solving

$$(\,K(x)\mathrm{Diag}(\mathbf{H}x + b) + \mathrm{Diag}(v(x))\,\mathbf{H}\,)\,p = -\mathrm{Diag}(v(x))\,(\mathbf{H}x + b)$$

for the update p at a given iterate x, followed by $x \leftarrow x + p$.

- **Each iteration entails the solution of a large linear system.**
- **Linear complexity, $\mathcal{O}(C)$, where C is the number of mesh cells.**
- **Conjecture: Parallelizes as well as multigrid $\rightarrow$ $\mathbf{DD}^T$ operator.**

Flux-form OBR speed in transport applications

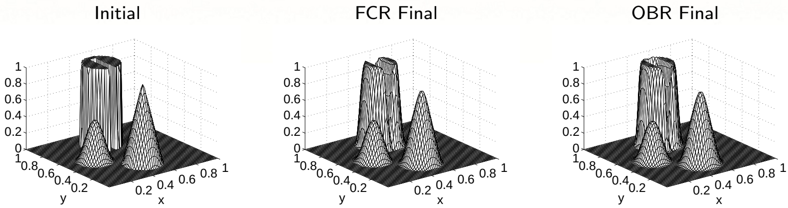

Figure: After one full revolution (810 time steps) on a 128×128 mesh.

mesh	steps	**FCR** time(sec)	**Flux-OBR** time(sec)	ratio
64×64	408	3.3	63.7	19.3
128×128	810	26.4	496.4	18.8
256×256	1614	229.1	3464.2	15.1

Table: Computational cost. **Flux-form OBR is not competitive!**

Solution transfer

Scalar mass-density remap

Flux form of optimization-based remap
- Mathematical formulation
- Theoretical properties and benefits
- Algorithm and computational cost

Mass form of optimization-based remap
- Mathematical formulation
- Algorithm and computational cost

New directions and technology transfer
- Adaptable targets and smoothness indicators
- High-order remap: BLAST, HOMME
- Tensor remap: ALEGRA

Mass form of OBR

1. Define **mass update**

$$\widetilde{m} = m + \delta m \,,$$

where δm approximates the exact **mass increments** between new and old cells:

$$\delta m_i \approx \delta m_i^{\text{exact}} = \int_{\widetilde{c}_i} \rho(\mathbf{x}) dV - \int_{c_i} \rho(\mathbf{x}) dV \,;$$

where $i = 1, \ldots, C$.

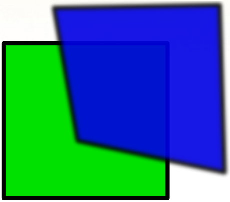

$\widetilde{m}_i = m_i + \delta m_i$

Note: $\delta m_i = (\mathbf{D}F)_i$

2. Compute **target** $\delta m_i^{\mathrm{T}} := \int_{\widetilde{c}_i} \rho^h(\mathbf{x}) dV - \int_{c_i} \rho^h(\mathbf{x}) dV, \;\; i = 1, \ldots, C$, for density $\rho^h(\mathbf{x})$ that is **exact for linear functions**. Solve:

$$\begin{cases} \underset{\delta m}{\text{minimize}} \quad \dfrac{1}{2} \| \delta m - \delta m^{\mathrm{T}} \|_{\ell_2}^2 \qquad \text{subject to} \\ \sum_{i=1}^{C} \delta m_i = 0 \quad \text{and} \quad \widetilde{m}^{\min} \leq m + \delta m \leq \widetilde{m}^{\max} \,. \end{cases}$$

Mass-form OBR algorithm

We solve

$$\begin{cases} \underset{\delta m}{\text{minimize}} \quad \frac{1}{2}\|\delta m - \delta m^{\mathrm{T}}\|_{\ell_2}^2 \qquad \text{subject to} \\ \sum_{i=1}^{C} \delta m_i = 0 \quad \text{and} \quad \widetilde{m}^{\min} \le m + \delta m \le \widetilde{m}^{\max}. \end{cases}$$

Known as the **singly linearly constrained QP with simple bounds**, see Dai, Fletcher (2006, Math. Program.).

Key observation: The related optimization problem without the mass conservation constraint, $\sum_{i=1}^{C} \delta m_i = 0$, is **fully separable**!

The related problem can be solved by independently (and concurrently) solving C **one-dimensional** quadratic programs with simple bounds.

Goal: Satisfy the second constraint, $\sum_{i=1}^{C} \delta m_i = 0$, "in a few iterations".

Mass-form OBR algorithm

We solve

$$\begin{cases} \underset{\delta m}{\text{minimize}} \quad \frac{1}{2}\|\delta m - \delta m^{\mathrm{T}}\|_{\ell_2}^2 \qquad \text{subject to} \\ \sum_{i=1}^{C} \delta m_i = 0 \quad \text{and} \quad \widetilde{m}^{\min} \leq m + \delta m \leq \widetilde{m}^{\max}. \end{cases}$$

Known as the **singly linearly constrained QP with simple bounds**, see Dai, Fletcher (2006, Math. Program.).

Key observation: The related optimization problem without the mass conservation constraint, $\sum_{i=1}^{C} \delta m_i = 0$, is **fully separable**!

The related problem can be solved by independently (and concurrently) solving C **one-dimensional** quadratic programs with simple bounds.

Goal: Satisfy the second constraint, $\sum_{i=1}^{C} \delta m_i = 0$, "in a few iterations".

Mass-form OBR algorithm

We solve

$$\begin{cases} \underset{\delta m}{\text{minimize}} \quad \frac{1}{2}\|\delta m - \delta m^{\mathrm{T}}\|_{\ell_2}^2 \qquad \text{subject to} \\ \sum_{i=1}^{C} \delta m_i = 0 \quad \text{and} \quad \widetilde{m}^{\min} \leq m + \delta m \leq \widetilde{m}^{\max} \,. \end{cases}$$

Known as the **singly linearly constrained QP with simple bounds**, see Dai, Fletcher (2006, Math. Program.).

Key observation: The related optimization problem without the mass conservation constraint, $\sum_{i=1}^{C} \delta m_i = 0$, is **fully separable**!

The related problem can be solved by independently (and concurrently) solving C **one-dimensional** quadratic programs with simple bounds.

Goal: Satisfy the second constraint, $\sum_{i=1}^{C} \delta m_i = 0$, "in a few iterations".

Mass-form OBR algorithm

Define Lagrangian functional $\mathcal{L} : \mathbb{R}^C \times \mathbb{R} \times \mathbb{R}^C \times \mathbb{R}^C \to \mathbb{R}$,

$$\mathcal{L}(\delta m, \lambda, \mu_1, \mu_2) = \frac{1}{2}\sum_{i=1}^{C}(\delta m_i - \delta m_i^{\mathrm{T}})^2 - \lambda \sum_{i=1}^{C} \delta m_i -$$

$$\sum_{i=1}^{C} \mu_{1,i}\left(\delta m_i - \widetilde{m}_i^{\min} + m_i\right) - \sum_{i=1}^{C} \mu_{2,i}\left(\widetilde{m}_i^{\max} - m_i - \delta m_i\right) \,,$$

where $\delta m \in \mathbb{R}^C$ are the primal optimization variables, and $\lambda \in \mathbb{R}$, $\mu_1 \in \mathbb{R}^C$, and $\mu_2 \in \mathbb{R}^C$ are the dual optimization variables.

KKT conditions:

$$\delta m_i = \delta m_i^{\mathrm{T}} + \lambda + \mu_{1,i} - \mu_{2,i}; \quad i = 1, \ldots, C$$

$$\widetilde{m}_i^{\min} - m_i \le \delta m_i \le \widetilde{m}_i^{\max} - m_i; \quad i = 1, \ldots, C$$

$$\mu_{1,i} \ge 0\,, \quad \mu_{2,i} \ge 0; \quad i = 1, \ldots, C$$

$$\mu_{1,i}\left(\delta m_i - \widetilde{m}_i^{\min} + m_i\right) = 0\,, \quad \mu_{2,i}\left(-\delta m_i + \widetilde{m}_i^{\max} - m_i\right) = 0; \quad i = 1, \ldots, C$$

$$\sum_{i=1}^{C} \delta m_i = 0$$

Mass-form OBR algorithm

We solve the KKT conditions directly.

First, we focus on the conditions in black, separable in the index i. For any *fixed* value of λ a solution to the "black" conditions is given by

$$\begin{cases} \delta m_i = \delta m_i^T + \lambda; & \mu_{1,i} = \mu_{2,i} = 0 & \text{if} \quad \widetilde{m}_i^{\min} - m_i \le \delta m_i^T + \lambda \le \widetilde{m}_i^{\max} - m_i \\ \delta m_i = \widetilde{m}_i^{\min} - m_i; & \mu_{2,i} = 0,\ \mu_{1,i} = \delta m_i - \delta m_i^T - \lambda & \text{if} \quad \delta m_i^T + \lambda < \widetilde{m}_i^{\min} - m_i \\ \delta m_i = \widetilde{m}_i^{\max} - m_i; & \mu_{1,i} = 0,\ \mu_{2,i} = \delta m_i^T - \delta m_i + \lambda & \text{if} \quad \delta m_i^T + \lambda > \widetilde{m}_i^{\max} - m_i\,, \end{cases}$$

for all $i = 1, \ldots, C$.

Ignoring μ_1 and μ_2 and treating δm_i as a function of λ yields

$$\delta m_i(\lambda) = \text{median}(\widetilde{m}_i^{\min} - m_i,\ \delta m_i^T + \lambda,\ \widetilde{m}_i^{\max} - m_i)\,, \qquad i = 1, \ldots, C\,.$$

This is a trivial, communication-free $\mathcal{O}(C)$ computation.

Mass-form OBR algorithm

Second, we adjust λ in an outer iteration in order to satisfy

$$\sum_{i=1}^{C} \delta m_i(\lambda) = 0\,.$$

When we find the λ^* such that $\sum_{i=1}^{C} \delta m_i(\lambda^*) = 0$ holds, we will have solved the full KKT conditions.

The function $\sum_{i=1}^{C} \delta m_i(\lambda)$ is a piecewise linear, monotonically increasing function of a single scalar variable λ. Therefore, a **secant method** can be efficiently employed as the outer iteration.

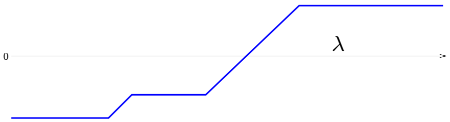

... given λ_p, λ_c, r_p

1. Compute $\delta m_i(\lambda_c) \leftarrow \text{median}(\widetilde{m}_i^{\text{min}} - m_i,\ \delta m_i^{\text{T}} + \lambda_c,\ \widetilde{m}_i^{\text{max}} - m_i)\ \forall i$.

   Compute residual $r_c \leftarrow \sum_{i=1}^{C} \delta m_i(\lambda_c)$.
2. Set $\alpha \leftarrow (\lambda_p - \lambda_c)/(r_p - r_c)$. Set $r_p \leftarrow r_c$.
3. Set $\lambda_p \leftarrow \lambda_c$. Set $\lambda_c \leftarrow \lambda_c - \alpha r_c$.

In all our examples, the algorithm requires ≤ 5 secant iterations!

Mass-form OBR speed in transport applications

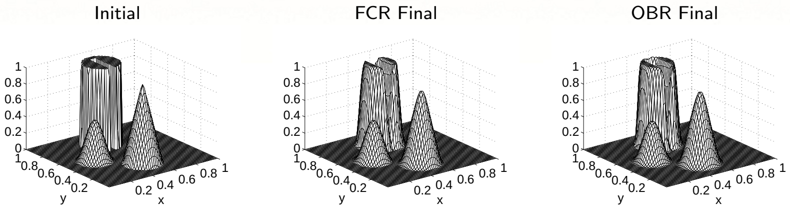

Figure: After one full revolution (810 time steps) on a 128×128 mesh.

mesh	steps	FCR time(sec)	Flux-OBR time(sec)	ratio	Mass-OBR time(sec)	ratio
64×64	408	3.3	63.7	19.3	3.4	1.0
128×128	810	26.4	496.4	18.8	26.2	1.0
256×256	1614	229.1	3464.2	15.1	222.7	1.0

Table: Computational cost. **Mass-form OBR is as fast as a local scheme!**

Adaptable targets

- Cost-function targets are built from the reconstruction:

$$\rho^h(\mathbf{x})|_{c_i} := \rho_i^h(\mathbf{x}) = \rho_i + \mathbf{g}_i \cdot (\mathbf{x} - \mathbf{b}_i) \quad \forall c_i \in C(\Omega)\,,$$

  where ρ_i are density values on the old cells c_i, $\mathbf{g}_i$ is a least-squares approximation of the gradient $\nabla\rho$ based on ρ_i from the cells in the neighborhood $N(c_i)$, and $\mathbf{b}_i$ is the barycenter of c_i.

- Define **reconstruction residual**: $q_i = \sum_{j \in N(c_i)} |\rho_j - \rho_i^h(\mathbf{b}_j)|\,.$

- Modify the gradient of $\rho^h(\mathbf{x})$ to obtain **adaptable reconstruction**:

$$\rho^A(\mathbf{x})|_{c_i} := \rho_i^A(\mathbf{x}) = \rho_i + \alpha_i(q_i)\mathbf{g}_i \cdot (\mathbf{x} - \mathbf{b}_i) \quad \forall c_i \in C(\Omega)\,.$$

- For a given constant $\gamma > 0$,

$$\alpha_i(q_i) = \begin{cases} 1 & \text{if “}\textit{smooth}\text{''} \\ 1 + \gamma\, q_i / \max\limits_{i=1,\dots,C}\{q_i\} & \text{otherwise}\,. \end{cases}$$

Dual variables as smoothness indicators

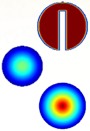

$$\begin{cases} \mu_{1,i} = \mu_{2,i} = 0 & \text{if} \quad \widetilde{m}_i^{\min} - m_i \le \delta m_i^{T} + \lambda \le \widetilde{m}_i^{\max} - m_i \\ \mu_{2,i} = 0,\ \mu_{1,i} = (\widetilde{m}_i^{\min} - m_i) - \delta m_i^{T} - \lambda & \text{if} \quad \delta m_i^{T} + \lambda < \widetilde{m}_i^{\min} - m_i \\ \mu_{1,i} = 0,\ \mu_{2,i} = \delta m_i^{T} - (\widetilde{m}_i^{\max} - m_i) + \lambda & \text{if} \quad \delta m_i^{T} + \lambda > \widetilde{m}_i^{\max} - m_i\,, \end{cases}$$

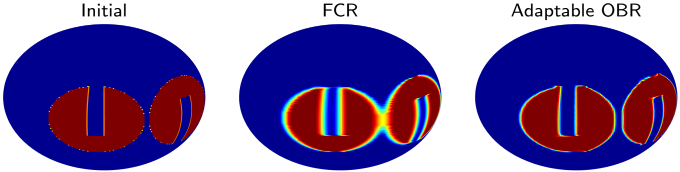

Figure: Transport results for the solid-body rotation test on the sphere, for two revolutions, left to right and back (1920 time steps) on a 0.75° mesh.

mesh	steps	FCR time(sec)	Mass-OBR time(sec)	ratio	FCR L_1 error	rate	Mass-OBR L_1 error	rate
3°	480	17.4	18.2	1.0	3.25e-2	—	2.79e-2	—
1.5°	960	132.5	151.6	1.1	1.99e-2	0.78	1.36e-3	1.04
0.75°	1920	1184.5	1379.0	1.2	1.10e-2	0.78	5.41e-3	1.18

Dual variables as smoothness indicators

$$
\begin{cases}
\mu_{1,i} = \mu_{2,i} = 0 & \text{if} \quad \widetilde{m}_i^{\min} - m_i \le \delta m_i^T + \lambda \le \widetilde{m}_i^{\max} - m_i \\
\mu_{2,i} = 0,\ \mu_{1,i} = (\widetilde{m}_i^{\min} - m_i) - \delta m_i^T - \lambda & \text{if} \quad \delta m_i^T + \lambda < \widetilde{m}_i^{\min} - m_i \\
\mu_{1,i} = 0,\ \mu_{2,i} = \delta m_i^T - (\widetilde{m}_i^{\max} - m_i) + \lambda & \text{if} \quad \delta m_i^T + \lambda > \widetilde{m}_i^{\max} - m_i\,,
\end{cases}
$$

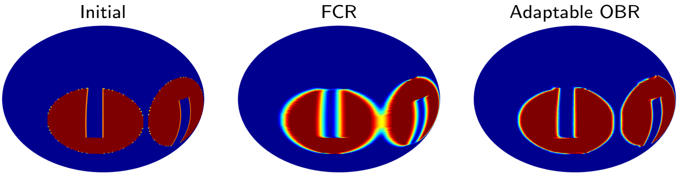

Figure: Transport results for the solid-body rotation test on the sphere, for two revolutions, left to right and back (1920 time steps) on a 0.75° mesh.

mesh	steps	**FCR** time(sec)	**Mass-OBR** time(sec)	ratio	**FCR** L_1 error	rate	**Mass-OBR** L_1 error	rate
3°	480	17.4	18.2	1.0	3.25e-2	—	2.79e-2	—
1.5°	960	132.5	151.6	1.1	1.99e-2	0.78	1.36e-3	1.04
0.75°	1920	1184.5	1379.0	1.2	1.10e-2	0.78	5.41e-3	1.18

Deformational Flow Test

For a more challenging test case we transport two notched cylinders initially centered at $(\lambda_1, \theta_1) = (5\pi/6, 0)$ and $(\lambda_2, \theta_2) = (7\pi/6, 0)$ in the following deformational velocity field

$$u(\lambda, \theta, t) = 2\sin^2\lambda \sin 2\theta \cos(\pi t/T)$$
$$v(\lambda, \theta, t) = 2\sin(2\lambda)\cos(\theta)\cos(\pi t/T)$$

with period $T = 5$. In this case an adaptable target is used with parameters $\gamma_1 = 0.1$ and $\gamma_2 = 0.5$, resulting in a sharper final density distribution and higher convergence rate than transport with Flux-Corrected Remap (FCR).

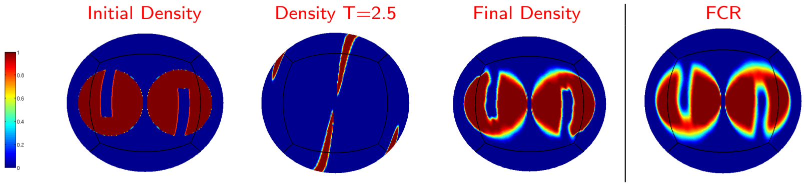

MVMT-a transport results for the deformational flow test on the sphere, shown at the time of maximum deformation (t = 2.5) and at the final time (t = 5) for a total of 2400 time steps on a mesh with 120x120 elements per panel. FCR results shown at right.

Elements per panel	# steps	**FCR** time(sec)	**MVMT-a** time(sec)	**FCR** L_1 error	rate	**MVMT-a** L_1 error	rate
30×30	600	45.9	46.3	5.59e-1	—	4.58e-1	—
60×60	1200	281.3	286.9	3.67e-1	0.61	2.49e-1	0.88
120×120	2400	2103.7	2140.3	2.19e-1	0.68	1.25e-1	0.94

Comparison of L_1 errors with respect to the initial condition for Flux-Corrected Remap (FCR) and MVMT-a and comparison of computational costs as measured by Matlab^{TM} wall-clock times in seconds, on a single Intel Xeon X5450 3.0GHz processor.

High-order remap

Software: **C**onstrained **O**ptimization **B**ased **R**emap **A**lgorithms

BLAST

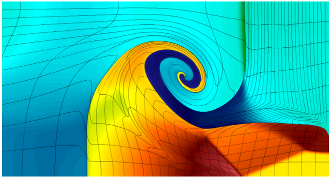

- Next-gen LLNL hydrocode.
- Mass-form OBR to enable conservative and (essentially) non-oscillatory high-order ALE.
- Integration of the COBRA library is in progress.
- Tzanio Kolev, et al.; LDRD.
- **Research:** Energy constraints.

HOMME

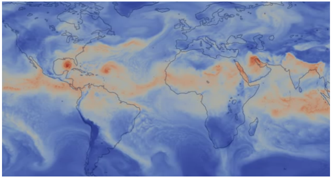

- The default dynamical core of the Community Atmosphere / Earth System Models.
- OBR to enable a very fast conservative and monotone semi-Lagrangian scheme.
- Mark Taylor, et al.; SciDAC 3.
- **Research:** Tracer transport.

Tensor remap

ALEGRA

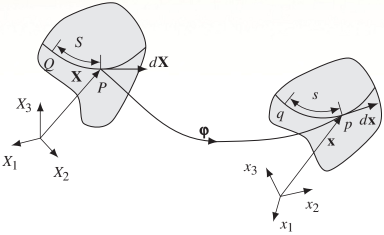

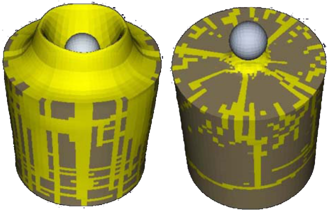

- Shock and multiphysics family of codes, including solid kinematics.
- **Challenge:** Solid kinematics schemes fail in presence of large deformations.
- **Cause:** Violation of physical constraints.
- **Deformation gradient:** $\mathbf{F} = \frac{\partial x_i}{\partial X_A} \mathbf{e}_i \otimes \mathbf{E}_A$.
- **Constraints — sparse but global:**

$$\operatorname{curl} \mathbf{F}^{-1} = \mathbf{0} \quad \text{and} \quad \det \mathbf{F} > 0 \,.$$

- Integrated interior-point methods from our Rapid Optimization Library into ALEGRA.
- Jim Kamm, Ed Love, et al.; ASC CSAR.
- **Much, much harder than scalar remap!**

Summary

- Traditional preservation of properties relies on mesh topology, variable placement, and local "worst-case scenarios" – imposes restrictions on mesh and/or accuracy
- Optimization-based approaches present an attractive alternative:
  - Accuracy is separated from the preservation of physical properties.
  - Physical properties can be treated as optimization constraints.
  - Discretization is relieved from securing these properties.
  - Solution is a globally optimal state: the best possible, with respect to the target state satisfying the constraints.
- Optimization-based remappers (OBR) are more robust and more accurate than explicit limiter-based remappers.
- The mass-form OBR algorithm is as fast as a local scheme.
- The optimization approach allows for specially tuned targets.
- Dual optimization variables may be used to tune targets.
- Multi-tracer transport can be done efficiently (in progress).
- Tensor remap (remap for solid deformation) needs real optimization.

Publications

- P. Bochev, D. Ridzal, K. Peterson, *Optimization-based remap and transport: A divide and conquer strategy for feature-preserving discretizations*, **J. Comput. Phys.**, In Press, 2013.
- J. R. Kamm, E. Love, A. C. Robinson, J. Young, D. Ridzal, *Edge Remap for Solids*, SAND report, Sandia National Laboratories, 2013.
- K. Peterson, P. Bochev, D. Ridzal, *Optimization-based conservative transport on the cubed-sphere grid*, in Proceedings of the 9th International Conference on Large-Scale Scientific Computations, Sozopol, Bulgaria (2013).
- P. Bochev, D. Ridzal, M. Shashkov, *Fast optimization-based conservative remap of scalar fields through aggregate mass transfer*, **J. Comput. Phys.**, 246:37–57, 2013.
- P. Bochev, D. Ridzal, G. Scovazzi, and M. Shashkov, *Constrained-optimization based data transfer: A new perspective on flux correction*, in **Flux-Corrected Transport**, edited by D. Kuzmin, R. Lohner, S. Turek, Springer-Verlag, 2012.
- P. Bochev, D. Ridzal, J. Young, *Optimization-Based Modeling with Applications to Transport. Part 1. Abstract Formulation.*, In: Lirkov, I., Margenov, S., Waśniewski, J. (eds.), LSSC 2011, **LNCS**, vol. 7116, pp. 63–71. Springer, Heidelberg (2012).
- P. Bochev, J. Young, D. Ridzal, *Optimization-Based Modeling with Applications to Transport. Part 2: The Optimization Algorithm*, In: Lirkov, I., Margenov, S., Waśniewski, J. (eds.), LSSC 2011, **LNCS**, vol. 7116, pp. 72–80. Springer, Heidelberg (2012).
- D. Ridzal, P. Bochev, J. Young, K. Peterson, *Optimization-Based Modeling with Applications to Transport. Part 3: Implementation and Computational Studies*, In: Lirkov, I., Margenov, S., Waśniewski, J. (eds.), LSSC 2011, **LNCS**, vol. 7116, pp. 81–88. Springer, Heidelberg (2012).
- P. Bochev, D. Ridzal, G. Scovazzi, and M. Shashkov, *Formulation, analysis and numerical study of an optimization-based conservative interpolation (remap) of scalar fields for arbitrary Lagrangian-Eulerian methods*, **J. Comput. Phys.**, 230(13):5199–5225, 2011.